Article published in International Journal of Solids and Structures 110–111 (2017), 15–23. The final publication is available at www.sciencedirect.com, doi:10.1016/j.ijsolstr.2017.02.007. The preprint contains corrections according to erratum (doi:10.1016/j.ijsolstr.2017.03.030).

A micromechanical gradient extension of Gurson's model of ductile damage within the theory of microdilatational media

Geralf Hütter

March 30, 2017

Gurson's model and its numerous modifications are established for simulating ductile failure. However, this model is formulated within the theory of simple materials which is why it predicts a localization of deformation within an infinitesimally thin band for the softening regime. Corresponding FEM simulations exhibit a spurious mesh dependency. In order to overcome this problem, several heuristic extensions of Gurson's model to non-local or gradient theories were proposed in literature. Although these extensions are computationally effective, the particular implementation and interpretation of the additional terms and the corresponding constitutive parameters is problematic. In contrast, the extension of Gurson's model by Gologanu et al. [12] (GLPD model) towards strain gradient media by homogenization does not have these problems but its numerical implementation is considerably more complicated.

The present contribution aims in providing a gradient extension of Gurson's model which combines computational efficiency with a sound micromechanical basis. For this purpose a theory of homogenization towards unconstrained microdilatational media is developed. Based on this theory, a limit-load analysis is performed for a unit cell with void leading to a closed-form yield function of Gurson-type which contains additional terms of the microdilatational theory.

Keywords: ductile damage; micromorphic theory; homogenization; generalized continua

1. Introduction

Ductile damage and the associated failure of components is critical in many engineering applications. The ductile mechanism consists of the nucleation, growth and coalescence of microscopic voids during plastic deformations. The constitutive model of Gurson [14, 15] and its numerous modifications are established to simulate the ductile damage and failure of components. For recent reviews, the reader is referred to [1, 2, 4]. The problem of Gurson's model, and actually of all damage models which are formulated within the framework of simple materials, is that they predict a localization of deformation within an infinitesimally thin band at the onset of macroscopic softening. This prediction is physically unrealistic and contradicts the basic assumptions of continuum mechanics, namely that the macroscopic gradients need to be negligible compared to characteristic length scales of the microstructure ("separation of scales"). Mathematically, the underlying boundary value problem becomes ill-posed and with decreasing element size, corresponding FE simulations converge only to a physically unrealistic infinitesimally thin band of localization, often termed a "spurious mesh-dependence". In reality, microstructural length scales limit the macroscopic gradients and thus determine the finite size of localization bands. For the ductile mechanism, the distance of voids or void nuclei forms this characteristic microstructural length scale. Thus, it was recognized that it is necessary to include the relevant microstructural length scale as *intrinsic length* into the macroscopic continuum description in order to "regularize" the boundary value problem in the softening regime. For this purpose, nonlocal [18, 21, 25] and gradient extensions of Gurson's model [22, 26] were proposed heuristically. In particular, so-called implicitly gradient enriched formulations turned out to be advantageous for numerical simulations as they can be implemented to available finite element codes without requiring any change to the global program but only a single additional nodal degree of freedom. However, due to their purely heuristic formulation, the interpretation of the additionally necessary boundary conditions is problematic. In addition, the heuristic nonlocal or gradient extensions were mostly introduced as linear terms which seems questionable in the context of the highly nonlinear Gurson model or other constitutive models of ductile damage.

In contrast, Gologanu et al. [12] extended Gurson's homogenization approach to the strain-gradient theory whereby it turned out that the additional gradient terms, and consequently the distance of voids as intrinsic length, enter the yield function and thus have indeed a highly non-linear contribution. Numerical results [3, 6] show that this model overcomes the aforementioned problems in principle. The problem with the model of [12] (GLPD model) is its cumbersome FE implementation. A strain gradient theory imposes stronger restrictions to the continuity which cannot be fulfill by standard polynomial shape functions. Even if this problem is circumvented by hybrid or penalty formulations, the computational effort raises dramatically since the complete strain tensor becomes a nodal variable[1].

To sum up the current state of ductile damage models which can handle localization, it can be said that one has to chose between computationally efficient but purely heuristic implicit-gradient enriched Gurson models [22, 26] or the micromechanically sound but computationally expensive strain-gradient GLPD model [12]. Comparing these approaches shows that both types are subclasses of generalized micromorphic continua in the sense of Forest [10]. The implicit-gradient enriched models postulate an additional PDE of balance type on the porosity, which drives the softening in Gurson's model, or the directly related dilatational strain, which is why they can be classified as microdilatational continua. The strain-gradient theory of Gologanu et al. [12] can be classified as a constrained micromorphic theory where microdeformation and macrodeformation are constrained to coincide.

It is the scope of the present contribution to combine the computational efficiency of implicit-gradient enriched models with the micromechanically sound basis of the GLPD model. For this purpose, Gurson's model shall be extended to the theory of unconstrained microdilatational media [11, 13] by homogenization. The present paper is organized as follows: In section 2 the general theory of homogenization towards micromorphic continua of Hütter [16] is confined to microdilatational media and adapted to a medium with voids, including the macroscopic balance equations, the extended Hill-Mandel lemma and the micro-macro relations for all involved kinematic and kinetic quantities. The particular microdilatational model for ductile damage is derived in section 3 by a limit load analysis for the plastic behavior and closed-form solutions for the homogenization of the elastic behavior. Section 4 discusses whether and how established heuristic extensions of Gurson's model can be adapted to the microdilatational model before section 5 closes with a short summary and outlook.

2. Homogenization towards a microdilatational continuum

In the symbolic tensor notation, scalars, vectors and tensors of second and third order are denoted by a, $\underline{\mathbf{b}}$, $\underset{\sim}{\mathbf{c}}$, $\underset{\approx}{\mathbf{d}}$, whose components in a Cartesian frame are a, b_i, c_{ij} and d_{ijk}, respectively. Single and double contractions of them are written as $\cdot$ and $:$, respectively, and are computed from left to right, e. g.

[1] The recently proposed technique by Bergheau et al. [3] requires fundamental modifications of the compilation of the global system of equations and is thus hardly suitable for standard multi-purpose FE codes.

$\underset{\sim}{\mathbf{c}} : \underset{\sim}{\mathbf{e}} = c_{ij}e_{ij}$. The dimension of space is $n = \delta_{kk}$ (2 or 3). Capital Latin letters refer to the macroscopic level whereas lowercase symbols denote microscopic quantities. In cases where this convention might be confusing, macroscopic quantities are labeled by an overbar. For instance, the macroscopic and microscopic location vectors are $\underline{\mathbf{X}}$ and $\underline{\mathbf{x}}$, respectively, whereas $\overline{\Phi}$ and Φ are the macroscopic and microscopic values of the specific intrinsic energy, respectively. The index of the nabla operator, $\underline{\nabla}_{\underline{\mathbf{x}}}$ or $\underline{\nabla}_{\underline{\mathbf{X}}}$, indicates whether it is computed with respect to the microscopic or the macroscopic location vector, respectively.

2.1. Averaging

For the homogenization procedure, it is useful to start with providing a general averaging procedure for transferring a general balance equations at the microscale of type

$$\rho\overset{\bullet}{\varphi}_m = \underline{\nabla}_{\underline{\mathbf{x}}} \cdot \underline{\psi}_a + \rho\psi_m \text{ in } \Omega\,. \tag{1}$$

to the macroscale. Therein, φ_m, $\underline{\psi}_a$ and ψ_m are general storage, flux and source densities, respectively, and ρ is the mass density. According to Eringen [7] (and outlined in [16]), macroscopic counterparts to these balance equations are obtained by dividing the domain Ω into small but finite subdomains $\Delta V(\underline{\mathbf{X}})$. Approximating the global sum of those many subdomains as an integral and application of Gauss' theorem leads to the macroscopic balance law

$$\langle\rho\overset{\bullet}{\varphi}_m\rangle_V = \underline{\nabla}_{\underline{\mathbf{X}}} \cdot \left\langle\underline{\psi}_a\right\rangle_\Delta + \langle\rho\psi_m\rangle_V \tag{2}$$

Therein, the volume averaging operator is denoted as

$$\langle(\circ)\rangle_V := \frac{1}{\Delta V(\underline{\mathbf{X}})} \int\limits_{\Delta V(\underline{\mathbf{X}})} (\circ)(\underline{\mathbf{x}}) \;\, \mathrm{d}V \tag{3}$$

and the surface operator was specified in [16] as

$$\langle(\circ)\rangle_\Delta := \frac{1}{\Delta V} \int\limits_{\partial\Delta V} \underline{\xi} \otimes \underline{\mathbf{n}} \cdot (\circ)\, \mathrm{d}S \tag{4}$$

wherein the relative location vector $\underline{\xi} = \underline{\mathbf{x}} - \underline{\mathbf{X}}$ was introduced as distance between macroscopic and microscopic locations and $\partial\Delta V$ denotes the boundary of ΔV. The macroscopic location is defined as the geometrical center $\underline{\mathbf{X}} = \langle\underline{\mathbf{x}}\rangle_V$ of ΔV.

2.2. Macroscopic balance equations

The macroscopic balance equations are obtained by applying the average procedure (2) to the relevant microscopic balance equations which are, for a Cauchy continuum at the microscale, those of energy, and linear and angular momentum (having incorporated already the balance of mass):

Energy: $$\rho\left(\Phi + \frac{1}{2}\underline{\mathbf{v}} \cdot \underline{\mathbf{v}}\right)^{\bullet} = \underline{\nabla}_{\underline{\mathbf{x}}} \cdot \left(\underset{\sim}{\sigma} \cdot \underline{\mathbf{v}}\right) - \underline{\nabla}_{\underline{\mathbf{x}}} \cdot \underline{\mathbf{q}} + \rho\underline{\mathbf{f}} \cdot \underline{\mathbf{v}} \tag{5}$$

Linear momentum: $$\underline{\nabla}_{\underline{\mathbf{x}}} \cdot \underset{\sim}{\sigma} + \rho\underline{\mathbf{f}} - \rho\underline{\dot{\mathbf{v}}} = 0 \tag{6}$$

Angular momentum: $$\underset{\sim}{\sigma}^{\mathrm{T}} = \underset{\sim}{\sigma} \tag{7}$$

Therein, Φ is the specific intrinsic energy and $\underset{\sim}{\sigma}$, $\underline{\mathbf{v}}$, $\underline{\mathbf{f}}$ and $\underline{\mathbf{q}}$ denote the stress, velocity, body force and heat flux, respectively.

In particular, the macroscopic energy balance as macroscopic counterpart to (5) reads

$$\left\langle \rho\dot{\Phi}\right\rangle_V + \left\langle \rho\left(\frac{1}{2}\underline{\mathbf{v}}\cdot\underline{\mathbf{v}}\right)^{\bullet}\right\rangle_V = \underline{\nabla}_{\underline{\mathbf{X}}}\cdot\langle \underset{\sim}{\sigma}\cdot\underline{\mathbf{v}}\rangle_\Delta - \underline{\nabla}_{\underline{\mathbf{X}}}\cdot\langle\underline{\mathbf{q}}\rangle_\Delta + \langle\rho\underline{\mathbf{f}}\cdot\underline{\mathbf{v}}\rangle_V \tag{8}$$

Within a first order micromorphic theory, the microscopic velocity field $\underline{\mathbf{v}}(\underline{\mathbf{x}})$ is replaced in (8) by the linear approximation

$$\tilde{\underline{\mathbf{v}}} = \underline{\mathbf{V}}(\underline{\mathbf{X}}) + \underset{\sim}{\dot{\chi}}(\underline{\mathbf{X}})\cdot(\underline{\mathbf{x}}-\underline{\mathbf{X}})\,. \tag{9}$$

For a microdilatational theory, the rate of microdeformation is taken to be purely spherical

$$\underset{\sim}{\dot{\chi}} = \frac{1}{n}\dot{\chi}\underset{\sim}{\mathbf{I}} \tag{10}$$

wherein $\dot{\chi}(\underline{\mathbf{X}})$ is the rate of microdilatation. The factor $1/n$ ($1/3$ in 3D or $1/2$ in 2D, resp.) is introduced for convenience only so that the work-conjugate stress is the hydrostatic stress and $\dot{\chi}$ corresponds to a dilatation. Thus, the macroscopic energy balance (8) becomes

$$\underbrace{\left\langle \rho\dot{\Phi}\right\rangle_V}_{=:\overline{\rho}\dot{\overline{\Phi}}} + \underbrace{\langle\rho\rangle_V}_{=:\overline{\rho}}\frac{1}{2}\left(\underline{\mathbf{V}}\cdot\underline{\mathbf{V}}\right)^{\bullet} + \underbrace{\left\langle\frac{1}{n^2}\rho r^2\right\rangle_V}_{=:\overline{\rho}I_r}\frac{1}{2}\left(\dot{\chi}^2\right)^{\bullet}$$

$$= \underline{\nabla}_{\underline{\mathbf{X}}}\cdot[\underbrace{\langle\underset{\sim}{\sigma}\rangle_\Delta}_{=:\underset{\sim}{\mathbf{\Sigma}}}\cdot\underline{\mathbf{V}} + \underbrace{\left\langle\frac{1}{n}\underset{\sim}{\sigma}\cdot\underline{\xi}\right\rangle_\Delta}_{=:\underline{\mathbf{M}}}\dot{\chi}] - \underline{\nabla}_{\underline{\mathbf{X}}}\cdot\underbrace{\langle\underline{\mathbf{q}}\rangle_\Delta}_{=:\underline{\mathbf{Q}}} + \underbrace{\langle\rho\underline{\mathbf{f}}\rangle_V}_{=:\overline{\rho}\underline{\overline{\mathbf{f}}}}\cdot\underline{\mathbf{V}} + \underbrace{\left\langle\frac{1}{n}\rho\underline{\mathbf{f}}\cdot\underline{\xi}\right\rangle_V}_{=:\overline{\rho}\overline{f}_{\mathrm{h}}}\dot{\chi} \tag{11}$$

and allows to define the macroscopic values of intrinsic energy, mass density, stress, body load and heat flux as $\overline{\Phi}$, $\overline{\rho}$, $\underset{\sim}{\mathbf{\Sigma}}$, $\underline{\overline{\mathbf{f}}}$ and $\underline{\mathbf{Q}}$, respectively, as labeled. In addition to these classical terms, the hyperstress vector $\underline{\mathbf{M}}$ and inertia terms and body loads, I_r and $\overline{f}_{\mathrm{h}}$, respectively, appear which are associated with the microdilatation χ. In (11), it was assumed for simplicity that the volume element ΔV is central symmetric so that its centers of mass and geometry coincide which is why the terms with $\langle\rho(\underline{\mathbf{x}}-\underline{\mathbf{X}})\rangle_V$ vanish. For a geometrically linear analysis, the macroscopic counterpart to the balance of mass is that the macroscopic density $\overline{\rho}$ and the moment of inertia $\overline{\rho}I_r$ are constant. For deriving a balance of internal energy, expressions for the divergences $\underline{\nabla}_{\underline{\mathbf{X}}}\cdot\underset{\sim}{\mathbf{\Sigma}}$ and $\underline{\nabla}_{\underline{\mathbf{X}}}\cdot\underline{\mathbf{M}}$ of the classical stress $\underset{\sim}{\mathbf{\Sigma}}$ and of the hyperstress $\underline{\mathbf{M}}$ are necessary to dissolve the bracket in the first term on the right hand-side of (11) (which corresponds to the macroscopic flux of mechanical work). Firstly, application of average procedure (2) to (7) yields the classical macroscopic balance of linear momentum

$$0 = \underline{\nabla}_{\underline{\mathbf{X}}}\cdot\underset{\sim}{\mathbf{\Sigma}} + \overline{\rho}\underline{\overline{\mathbf{f}}} - \overline{\rho}\dot{\underline{\mathbf{V}}}\,. \tag{12}$$

The balance of linear momentum (6) weighted by $\underline{\mathbf{x}}$ exhibits also the structure of a balance equation (1). Together with (12), a macroscopic counterpart

$$0 = \underline{\nabla}_{\underline{\mathbf{X}}}\cdot\underbrace{\left\langle\frac{1}{n}\underset{\sim}{\sigma}\cdot(\underline{\mathbf{x}}-\underline{\mathbf{X}})\right\rangle_\Delta}_{=\underline{\mathbf{M}}} - \underbrace{\frac{1}{n}\left[\langle\underset{\sim}{\sigma}\rangle_V - \underset{\sim}{\mathbf{\Sigma}}\right]:\underset{\sim}{\mathbf{I}}}_{:=s} + \underbrace{\left\langle\frac{1}{n}\rho\underline{\mathbf{f}}\cdot(\underline{\mathbf{x}}-\underline{\mathbf{X}})\right\rangle_V}_{=\overline{\rho}\overline{f}_{\mathrm{h}}} - \underbrace{\left\langle\frac{1}{n^2}\rho r^2\right\rangle_V}_{=\overline{\rho}I_r}\ddot{\chi} \tag{13}$$

can be derived which relates the divergence of the hyperstress $\underline{\mathbf{M}}$ to the difference stress s and corresponding body forces and inertia terms (cf. [16]). Eq. (13) can be interpreted such that, in absence of body forces and inertia, the difference s between the hydrostatic parts of macroscopic stress $\underset{\sim}{\mathbf{\Sigma}}$ and average stress $\langle\underset{\sim}{\sigma}\rangle_V$ is the "source" of hyperstresses $\underset{\sim}{\underline{\mathbf{M}}}$. Furthermore, the balance of angular momentum requires the macroscopic stress to be symmetric

$$\underset{\sim}{\mathbf{\Sigma}}^{\mathrm{T}} = \underset{\sim}{\mathbf{\Sigma}}\,. \tag{14}$$

Inserting (12), (13) and (14) into (11) yields the balance of internal energy as

$$\overline{\rho}\dot{\overline{\Phi}} = \underset{\sim}{\mathbf{\Sigma}} : \underset{\sim}{\mathbf{D}} + s\dot{\chi} + \underline{\mathbf{M}} \cdot \dot{\underline{\mathbf{K}}} - \underline{\nabla}_{\underline{\mathbf{X}}} \cdot \underline{\mathbf{Q}} \tag{15}$$

whereby the macroscopic rates of deformation were introduced as[2]

$$\underset{\sim}{\mathbf{D}} = \left(\underline{\nabla}_{\underline{\mathbf{X}}} \underline{\mathbf{V}}\right)^{\mathrm{S}}, \qquad \dot{\underline{\mathbf{K}}} = \underline{\nabla}_{\underline{\mathbf{X}}} \dot{\chi}\,. \tag{16}$$

2.3. Thermodynamic considerations

If the continuum at the microlevel is a Coleman-Noll continuum so that the specific internal energy $\Phi(\underset{\sim}{\varepsilon}, \eta, h)$ as a function of strain, specific entropy and intrinsic variables, respectively, is a potential for stress $\underset{\sim}{\sigma}$ and temperature θ, i. e. $\theta = \partial\Phi/\partial\eta$ and $\underset{\sim}{\sigma} = \rho\partial\Phi/\partial\underset{\sim}{\varepsilon}$, the microscopic energy balance (5) reduces to $\rho D - \rho\theta\dot{\eta} = \underline{\nabla}_{\underline{\mathbf{x}}} \cdot \underline{\mathbf{q}}$. This equation is also of balance type and its macroscopic counterpart according to (2) can be used to eliminate the heat flux from the balance (15) of internal energy yielding

$$\left\langle \rho\dot{\Phi} \right\rangle_V = \overline{\rho}\dot{\overline{\Phi}} = \underset{\sim}{\mathbf{\Sigma}} : \underset{\sim}{\mathbf{D}} + s\dot{\chi} + \underline{\mathbf{M}} \cdot \dot{\underline{\mathbf{K}}} + \overline{\rho}\Theta\dot{S} - \underbrace{\langle \rho D \rangle_V}_{=:\overline{\rho}\overline{D}}\,. \tag{17}$$

Therein, $\overline{\rho}\overline{D}$ is the microscopic dissipation due to change of intrinsic variables which implies a corresponding definition of the macroscopic dissipation $\overline{D}$ in (17). Applying the chain rule for the functional dependencies of the intrinsic energy $\Phi(\underset{\sim}{\varepsilon}, \eta, h)$ on the left-hand side of (17), the dissipation and entropy terms drop out and what remains is a generalized Hill-Mandel lemma

$$\left\langle \underset{\sim}{\sigma} : \dot{\underset{\sim}{\varepsilon}} \right\rangle_V = \underset{\sim}{\mathbf{\Sigma}} : \underset{\sim}{\mathbf{D}} + s\dot{\chi} + \underline{\mathbf{M}} \cdot \dot{\underline{\mathbf{K}}}\,. \tag{18}$$

2.4. Micro-macro relations for compact material

For a fully micromorphic theory, i. e. with arbitrary microdeformation tensor $\dot{\underset{\sim}{\chi}}$, the kinematic micro-macro relations were established in [16] for a compact domain ΔV as

$$\underline{\mathbf{V}} = \langle \underline{\mathbf{v}} \rangle_V \tag{19}$$

$$\underline{\nabla}_{\underline{\mathbf{X}}} \underline{\mathbf{V}} = \left\langle \underline{\nabla}_{\underline{\mathbf{x}}} \underline{\mathbf{v}} \right\rangle_V \tag{20}$$

$$\dot{\underset{\sim}{\chi}} = \langle \underline{\mathbf{v}} \otimes \underline{\xi} \rangle_V \cdot \underset{\sim}{\mathbf{G}}^{-1} \tag{21}$$

$$\dot{\overline{K}}_{ijk} = \frac{1}{2}\left(\frac{\partial\dot{\chi}_{ij}}{\partial X_k} + \frac{\partial\dot{\chi}_{kj}}{\partial X_i}\right) = \frac{1}{2}\left[\frac{1}{2}\langle v_{j,i}\xi_m \rangle_V G^{-1}_{mk} + \frac{1}{2}\langle v_{j,k}\xi_m \rangle_V G^{-1}_{mi} - \frac{1}{2+n}\langle v_{j,m}\xi_m \rangle_V G^{-1}_{ik}\right] \tag{22}$$

whereby $\underset{\sim}{\mathbf{G}} = \left\langle \underline{\xi} \otimes \underline{\xi} \right\rangle_V$ refers to the second geometric moment. For a microdilatational theory, it is required that the rate of microdeformation $\dot{\underset{\sim}{\chi}}$ is spherical according to (10). Thus, the non-classical relations (21) and (22) become with (16)

$$\dot{\underset{\sim}{\chi}} = \frac{1}{n}\dot{\chi}\underset{\sim}{\mathbf{I}} \tag{23}$$

$$\dot{\overline{\underset{\sim}{\mathbf{K}}}} = \frac{1}{2n}\left(\underset{\sim}{\mathbf{I}} \otimes \dot{\underline{\mathbf{K}}} + \dot{\underline{\mathbf{K}}} \otimes \underset{\sim}{\mathbf{I}}\right)\,. \tag{24}$$

[2] Note that the choice of objective rates of deformation, and thus of their work conjugate stresses, differs in literature, e. g. between Eringen at al. [8] and Forest et al. [11]. The present choice is adapted to Eringen. Alternatively and equivalently, Forest et al. [11] choose $\underset{\sim}{\mathbf{D}}$, $\dot{\underline{\mathbf{K}}}$ and $\dot{\underset{\sim}{e}} := \underset{\sim}{\mathbf{D}} : \underset{\sim}{\mathbf{I}} - \dot{\underset{\sim}{\chi}}$ whose work-conjugate stresses in (15) would be $\bar{\underset{\sim}{\sigma}} := \underset{\sim}{\mathbf{\Sigma}} + \mathbf{s}\underset{\sim}{\mathbf{I}}$, $\underline{\mathbf{M}}$ and $\bar{s} := -s$, respectively. Within the homogenization procedure of [16], the former is identified as $\bar{\underset{\sim}{\sigma}} = \langle \underset{\sim}{\sigma} \rangle_V$, compare (13).

By equating these expressions to (21) and (22), the kinematic micro-macro relations of the microdilatational theory are found as

$$
\begin{aligned}
\dot{\chi} &= \underset{\sim}{\dot{\chi}} : \underset{\sim}{\mathbf{I}} = \langle \underline{\mathbf{v}} \otimes \underline{\xi} \rangle_V : \underset{\sim}{\mathbf{G}}^{-1} && (25)\\
\dot{K}_i &= \frac{n}{1+n}\left(\dot{K}_{ijj} + \dot{K}_{jji}\right) = \frac{n}{2(1+n)}\left[\langle v_{j,i}\xi_m\rangle_V\, G^{-1}_{mj} + \langle v_{j,j}\xi_m\rangle_V\, G^{-1}_{mi} - \frac{2}{2+n}\langle v_{j,m}\xi_m\rangle_V\, G^{-1}_{ij}\right] && (26)
\end{aligned}
$$

In contrast to the classical kinematic micro-macro relation (20), the volume averages $\langle(\circ)\rangle_V$ in the additional microdilatational relations (25) and (26) cannot be transformed completely to surface integrals which is why they cannot be prescribed uniquely to the microscopic volume $\Delta V(\underline{\mathbf{X}})$ by kinematic boundary conditions. Thus, the concept of minimal loading conditions proposed by Jänicke and Steeb [19] is employed as in [16] to fulfill the kinematic micro-macro relations (20), (25) and (26). If the material at the microscale is elastic, it is implemented into the principle of minimum potential energy via Lagrange multipliers as

$$
\begin{aligned}
\mathcal{L} = &\left\langle W(\underset{\sim}{\varepsilon})\right\rangle_V + \underline{\lambda}_U \cdot (\underline{\mathbf{U}} - \langle\underline{\mathbf{u}}\rangle_V) + \underset{\sim}{\lambda}_{\nabla U} : \left(\underline{\nabla}_{\underline{\mathbf{X}}}\underline{\mathbf{U}} - \left\langle \underline{\nabla}_{\underline{\mathbf{x}}}\underline{\mathbf{u}}\right\rangle_V\right) + \lambda_\chi\left(\chi - \left\langle \langle \underline{\mathbf{u}} \otimes \underline{\xi}\rangle_V : \underset{\sim}{\mathbf{G}}^{-1}\right\rangle_V\right)\\
&+ \underline{\lambda}_K \cdot \left\{\underline{\mathbf{K}} - \frac{n}{2(1+n)}\left[\left\langle \underline{\nabla}_{\underline{\mathbf{x}}}\underline{\mathbf{u}}\underline{\xi}\right\rangle_V : \underset{\sim}{\mathbf{G}}^{-1} + \left\langle \underline{\nabla}_{\underline{\mathbf{x}}} \cdot \underline{\mathbf{u}}\underline{\xi}\right\rangle_V \cdot \underset{\sim}{\mathbf{G}}^{-1} - \frac{2}{2+n}\left\langle \underline{\xi} \cdot \underline{\nabla}_{\underline{\mathbf{x}}}\underline{\mathbf{u}}\right\rangle_V \cdot \underset{\sim}{\mathbf{G}}^{-1}\right]\right\} \to \text{Min.}
\end{aligned}
\tag{27}
$$

whereby (19), (20), (25) and (26) were translated to displacements $\underline{\mathbf{u}}$. The corresponding stationarity conditions are the kinematic micro-macro relations and

$$
\begin{aligned}
\delta\mathcal{L} = 0 = &\left\langle \underset{\sim}{\sigma} : \delta\underset{\sim}{\varepsilon}\right\rangle_V - \underline{\lambda}_U \cdot \langle \delta\underline{\mathbf{u}}\rangle_V - \underset{\sim}{\lambda}_{\nabla U} : \left\langle \underline{\nabla}_{\underline{\mathbf{x}}}\delta\underline{\mathbf{u}}\right\rangle_V - \lambda_\chi \left\langle \langle \delta\underline{\mathbf{u}} \otimes \underline{\xi}\rangle_V : \underset{\sim}{\mathbf{G}}^{-1}\right\rangle_V\\
&- \underline{\lambda}_K \cdot \left[\left\langle \underline{\nabla}_{\underline{\mathbf{x}}}\delta\underline{\mathbf{u}}\underline{\xi}\right\rangle_V : \underset{\sim}{\mathbf{G}}^{-1} + \left\langle \underline{\nabla}_{\underline{\mathbf{x}}} \cdot \delta\underline{\mathbf{u}}\underline{\xi}\right\rangle_V \cdot \underset{\sim}{\mathbf{G}}^{-1} - \frac{2}{2+n}\left\langle \underline{\xi} \cdot \underline{\nabla}_{\underline{\mathbf{x}}}\delta\underline{\mathbf{u}}\right\rangle_V \cdot \underset{\sim}{\mathbf{G}}^{-1}\right]\frac{n}{2(1+n)}\,.
\end{aligned}
\tag{28}
$$

The stationarity condition (28) can be generalized to hold also for inelastic material if the variation $\delta\underline{\mathbf{u}}$ is interpreted as kinematically admissible test field ("virtual displacements"). Among those kinematically admissible fields is the actual velocity field $\underline{\mathbf{v}}(\underline{\mathbf{x}})$. Inserting it to (28) and comparing it with the generalized Hill-Mandel lemma (18) in the light of the kinematic micro-macro relations (20), (25) and (26), shows that the Lagrange multipliers correspond to the respective work-conjugate macroscopic stress measures

$$
\underset{\sim}{\lambda}_{\nabla U} = \underset{\sim}{\mathbf{\Sigma}}, \qquad \lambda_\chi = s, \qquad \underline{\lambda}_{\nabla\chi} = \underline{\mathbf{M}} \tag{29}
$$

and $\underline{\lambda}_U = 0$. With this substitution, the Euler-Lagrange equations to (28) read

$$
\begin{aligned}
\underline{\nabla}_{\underline{\mathbf{x}}} \cdot \underset{\sim}{\sigma} &= \frac{2n}{(1+n)(2+n)}\underline{\mathbf{M}} \cdot \underset{\sim}{\mathbf{G}}^{-1} - s\underline{\xi} \cdot \underset{\sim}{\mathbf{G}}^{-1} \text{ and } \underset{\sim}{\sigma} = \underset{\sim}{\sigma}^{\mathrm{T}} && \text{in } \Delta V(\underline{\mathbf{X}}) && (30)\\
\underset{\sim}{\sigma} \cdot \underline{\mathbf{n}} &= \underset{\sim}{\mathbf{\Sigma}} \cdot \underline{\mathbf{n}} + \frac{n}{2(1+n)}\underline{\mathbf{n}} \cdot \left[\underline{\mathbf{M}}\,\underline{\xi} \cdot \underset{\sim}{\mathbf{G}}^{-1} + \underset{\sim}{\mathbf{I}}\underline{\xi} \cdot \underset{\sim}{\mathbf{G}}^{-1} \cdot \underline{\mathbf{M}} - \frac{2}{2+n}\underline{\xi}\,\underset{\sim}{\mathbf{G}}^{-1} \cdot \underline{\mathbf{M}}\right] && \text{on } \partial\Delta V(\underline{\mathbf{X}}) && (31)
\end{aligned}
$$

The term $\underset{\sim}{\mathbf{\Sigma}}$ in the natural boundary condition (31) corresponds to the static boundary conditions in classical homogenization. Regarding the additional microdilatational terms, the difference stress s enters the PDE (30) and the hyper stress $\underline{\mathbf{M}}$ contributes to the tractions (31), both being linearly dependent of the relative location $\underline{\xi}$. Furthermore, $\underline{\mathbf{M}}$ appears in the volume (30) as a source term which is necessary for the fields to be self-equilibrating. The latter condition requires furthermore that the macroscopic stress $\underset{\sim}{\mathbf{\Sigma}}$ is symmetric according to (14).

Note that inserting (30), (31) into the definitions of the macroscopic stress measures $\underset{\sim}{\mathbf{\Sigma}}$, s and $\underline{\mathbf{M}}$ according to (11) and (13) in terms of the surface operator (4) leads to identities rendering the theory consistent.

Alternatively to (31), kinematic boundary conditions can be described which then have to fulfill the respective parts of the kinematic micro-macro relations ad-hoc. Inserting (24) to the kinematic boundary conditions derived in [16] for a fully micromorphic theory yields

$$\underline{\mathbf{v}} = \underline{\xi} \cdot \underline{\nabla_{\mathbf{X}} \mathbf{V}} + \frac{1}{n} \underline{\xi} \underline{\dot{\mathbf{K}}} \cdot \underline{\xi} + \frac{1}{2+n} \underline{\mathbf{V}} \underset{\sim}{\mathbf{G}}^{-1} : \left(\underline{\xi} \otimes \underline{\xi}\right) \qquad \text{on } \partial \Delta V(\underline{\mathbf{X}}) \tag{32}$$

which contains, in addition to the classical one, quadratic terms with $\underline{\dot{\mathbf{K}}}$. It can be verified that (32) fulfills the kinematic micro-macro relations (20) and (26) for $\underline{\nabla_{\mathbf{X}} \mathbf{V}}$ and $\underline{\dot{\mathbf{K}}}$. In contrast, the micro-macro relations (19) and (21) for the velocity $\underline{\mathbf{V}}$ and microdilatation χ cannot be transformed to surface integrals and thus not be prescribed by boundary conditions. Instead, (19) and (21) still need to be enforced by Lagrange multipliers as in (27) or (28), respectively.

2.5. Micro-macro relations for porous material

Let us consider a volume element $\Delta V = V_{\text{mat}} \cap V_{\text{void}}$ composed of matrix material $\underline{\mathbf{x}} \in V_{\text{mat}}$ and voids $\underline{\mathbf{x}} \in V_{\text{void}}$, the latter having a volume fraction of $f = V_{\text{void}}/\Delta V$. In classical homogenization, the only kinematic micro-macro relation (20) can be transformed to a surface integral

$$\underline{\nabla_{\mathbf{X}} \mathbf{V}} = \frac{1}{\Delta V(\underline{\mathbf{X}})} \oint_{\partial \Delta V(\underline{\mathbf{X}})} \underline{\mathbf{n}} \otimes \underline{\mathbf{v}} \, \mathrm{d}S \tag{33}$$

For this reason, the microscopic velocity field $\underline{\mathbf{v}}(\underline{\mathbf{x}})$ needs to be uniquely defined only on $\partial \Delta V(\underline{\mathbf{X}})$ which is unproblematic if the boundary is in the matrix only, i. e. $\partial \Delta V(\underline{\mathbf{X}}) \cap V_{\text{void}} = \emptyset$. In contrast, the microdilatational micro-macro relations (25) and (26) cannot be transformed completely to surface integrals. That is why it these relations need to be enforced globally requiring, however, that $\underline{\mathbf{v}}(\underline{\mathbf{x}})$ is well-defined in the complete domain ΔV. Unfortunately, in a porous material, the velocity field $\underline{\mathbf{v}}(\underline{\mathbf{x}})$ cannot uniquely be defined in the voids so that (25) and (26) cannot be applied in their present form. Nevertheless, it can unambiguously be assumed that the stress field $\underset{\sim}{\sigma} = 0$ vanishes in a void. If the void is furthermore associated with a vanishing mass density $\rho = 0$ and heat flux $\underline{\mathbf{q}} = 0$, even all microscopic balance equations (5)–(7) remain valid in the void. Consequently, the homogenization procedure outlined in sections 2.1–2.2 holds also for porous material, including in particular the micro-macro relations (11) and (13) for the stress measures $\underset{\sim}{\boldsymbol{\Sigma}}$, s and $\underline{\mathbf{M}}$. Thus, what is to be adapted to porous material are the kinematic relations (25) and (26). The fact that the kinematic relations in their present form are not suitable to porous material is reflected also in the fact that s and $\underline{\mathbf{M}}$, in their role as Lagrange multipliers to enforce (25) and (26), act as microscopic volume forces in (30) which cannot be carried by a void with $\underset{\sim}{\sigma} = 0$. Within the minimum loading conditions concept according to eqs. (27) and (28), respectively, these volume forces occur only since the voids V_{void} are part of the averaging domain ΔV in (27) and (28). Vice versa this means that the voids have to be excluded from the averaging domain. For this purpose, an matrix averaging operator is defined as

$$\langle (\circ) \rangle_{\text{M}} = \frac{1}{\Delta V} \int_{V_{\text{mat}}} (\circ) \, \mathrm{d}V \, . \tag{34}$$

Furthermore, (30) needs to be adapted to remain compatible with the kinetic micro-macro relations (13) for s and $\underline{\mathbf{M}}$. In the context of the minimum boundary condition concept, this requires for the linear term in (30) that the microdilatation be defined as

$$\dot{\chi} = \left\langle \underline{\mathbf{v}} \otimes \underline{\xi} \right\rangle_{\text{M}} : \underset{\sim}{\mathbf{G}}_{\text{M}}{}^{-1} \tag{35}$$

$$\underline{\dot{\mathbf{K}}} = \frac{2n}{1+n} \left[\frac{1}{4 \Delta V(\underline{\mathbf{X}})} \oint_{\partial \Omega} \underline{\mathbf{n}} \, \underline{\mathbf{v}} \, \underline{\xi} : \underset{\sim}{\mathbf{G}}^{-1} + \underline{\mathbf{n}} \cdot \underline{\mathbf{v}} \, \underline{\xi} \cdot \underset{\sim}{\mathbf{G}}^{-1} - \frac{2}{2+n} \underline{\mathbf{n}} \cdot \underline{\xi} \, \underline{\mathbf{v}} \cdot \underset{\sim}{\mathbf{G}}^{-1} \, \mathrm{d}S - \frac{1}{2+n} \underline{\mathbf{V}} \cdot \underset{\sim}{\mathbf{G}}^{-1} \right] \tag{36}$$

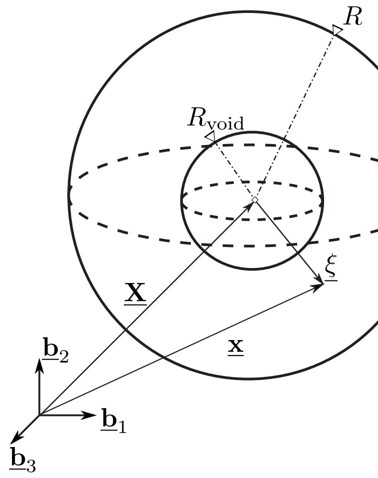

Figure 1: Spherical volume element with void

with the geometric moment of the matrix being $\underset{\sim}{\mathbf{G}}_{\mathrm{M}} = \left\langle \underline{\xi}\, \underline{\xi} \right\rangle_{\mathrm{M}}$. Furthermore, definitions (35) and (36) require $\left\langle \underline{\xi} \right\rangle_{\mathrm{M}} = 0$, which is fulfilled if the matrix material exhibits a central symmetry. In (36) the macroscopic velocity needs to be defined as

$$\underline{\mathbf{V}} = \frac{1}{1-f} \left\langle \underline{\mathbf{v}} \right\rangle_{\mathrm{M}} \,. \tag{37}$$

As envisaged, the kinematic micro-macro relations (35)–(37) encompass the microscopic velocity field $\underline{\mathbf{v}}(\underline{\mathbf{x}})$ in the matrix only, which is well-defined and so are the macroscopic kinematic quantities $\dot{\chi}$, $\dot{\underline{\mathbf{K}}}$ and $\underline{\mathbf{V}}$. Consequently, if these kinematic micro-macro relations are enforced by Lagrange multipliers as in eqs. (27) and (28), the local equilibrium condition (30) as Euler-Lagrange equation becomes

$$\underline{\nabla}_{\underline{\mathbf{x}}} \cdot \underset{\sim}{\sigma} = \begin{cases} \frac{1}{1-f} \frac{2n}{(1+n)(2+n)} \underline{\mathbf{M}} \cdot \underset{\sim}{\mathbf{G}}^{-1} - s \underline{\xi} \cdot \underset{\sim}{\mathbf{G}}_{\mathrm{M}}^{-1} & \underline{\mathbf{x}} \in V_{\mathrm{mat}} \\ 0 & \underline{\mathbf{x}} \in V_{\mathrm{void}} \end{cases} \tag{38}$$

which has no volume contributions in the void V_{void}. The natural or essential boundary conditions, (31) or (32), respectively, remain valid if the macroscopic velocity is defined as (37). It can be verified, that in this case and with (38), the kinetic micro-macro relations (11) and (13) for the stress measures $\underset{\sim}{\mathbf{\Sigma}}$, $\underline{\mathbf{M}}$ and s are fulfilled identically.

2.6. Spherical volume element with pore

In particular, a spherical void of radius R_{void} in a spherical volume element of radius R is considered, see Figure 1. For this special case, the microscopic volume and the void volume fraction are $\Delta V = 4\pi/3R^3$ and $f = (R_{\mathrm{void}}/R)^3$, respectively. The volume average operator (3) can favorably be written as [1]

$$\left\langle (\circ) \right\rangle_V = \frac{3}{R^3} \int_0^R r^2 \left\langle (\circ) \right\rangle_{S(r)} \mathrm{d}r \tag{39}$$

wherein $\left\langle (\circ) \right\rangle_{S(r)}$ denotes the arithmetic average over a spherical surface of radius $r = |\underline{\xi}|$. The expression for the average $\left\langle (\circ) \right\rangle_{\mathrm{M}}$ over the matrix material is (39) with the lower limit of the integral replaced by

R_{void}. Furthermore, the geometric moments of the complete $\Delta V(\underline{\mathbf{X}})$ and of the matrix are obtained as

$$\underset{\sim}{\mathbf{G}} = \langle \underline{\xi} \otimes \underline{\xi} \rangle_V = \frac{R^2}{5} \underset{\sim}{\mathbf{I}}, \qquad \underset{\sim}{\mathbf{G}}_{\mathrm{M}} = \langle \underline{\xi} \otimes \underline{\xi} \rangle_{\mathrm{M}} = \frac{1 - f^{5/3}}{5} R^2 \underset{\sim}{\mathbf{I}}, \tag{40}$$

respectively. Thus, the kinematic micro-macro relations (35) and (36) simplify to

$$\dot{\chi} = \frac{5}{(1 - f^{5/3}) R^2} \langle \underline{\mathbf{v}} \cdot \underline{\xi} \rangle_{\mathrm{M}} \tag{41}$$

$$\dot{\underline{\mathbf{K}}} = \frac{3}{2R^2} \left[\frac{3}{2} \langle 5 \underline{\mathbf{b}}_r \, \underline{\mathbf{v}} \cdot \underline{\mathbf{b}}_r - \underline{\mathbf{v}} \rangle_{S(R)} - \underline{\mathbf{V}} \right] \tag{42}$$

whereby it was used that for the boundary of the spherical cell, the normal $\underline{\mathbf{n}}$ coincides with the radial unit vector $\underline{\mathbf{b}}_r = \underline{\xi}/R = \underline{\mathbf{n}}$. The kinematic boundary condition (32) becomes

$$\underline{\mathbf{v}} = \underline{\xi} \cdot \nabla_{\underline{\mathbf{X}}} \underline{\mathbf{V}} + \frac{1}{3} \underline{\xi} \dot{\underline{\mathbf{K}}} \cdot \underline{\xi} + \underline{\mathbf{V}} \qquad \text{on } r = R. \tag{43}$$

3. Microdilatational constitutive law of ductile material

3.1. Elastic-plastic material

As in classical elastic-plastic theory, all macroscopic deformation measures are split into elastic and plastic parts

$$\underset{\sim}{\mathbf{E}} = \underset{\sim}{\mathbf{E}}_{\mathrm{el}} + \underset{\sim}{\mathbf{E}}_{\mathrm{pl}}, \qquad \chi = \chi_{\mathrm{el}} + \chi_{\mathrm{pl}}, \qquad \underline{\mathbf{K}} = \underline{\mathbf{K}}_{\mathrm{el}} + \underline{\mathbf{K}}_{\mathrm{pl}} \tag{44}$$

whereby the plastic parts $\underset{\sim}{\mathbf{E}}_{\mathrm{pl}}$, χ_{pl} and $\underline{\mathbf{K}}_{\mathrm{pl}}$ become macroscopic intrinsic variables. Subsequently, it is assumed that the intrinsic energy depends on the elastic parts only as well as on entropy S (and, potentially, on further intrinsic variables which describe the hardening behavior):

$$\overline{\Phi} = \overline{\Phi}(\underset{\sim}{\mathbf{E}}_{\mathrm{el}}, \chi_{\mathrm{el}}, \underline{\mathbf{K}}_{\mathrm{el}}, S)\,. \tag{45}$$

Thus, the work conjugate stresses are obtained according to (17) as

$$\underset{\sim}{\mathbf{\Sigma}} = \overline{\rho} \frac{\partial \overline{\Phi}}{\partial \underset{\sim}{\mathbf{E}}} = \overline{\rho} \frac{\partial \overline{\Phi}}{\partial \underset{\sim}{\mathbf{E}}_{\mathrm{el}}}, \qquad s = \overline{\rho} \frac{\partial \overline{\Phi}}{\partial \chi} = \overline{\rho} \frac{\partial \overline{\Phi}}{\partial \chi_{\mathrm{el}}}, \qquad \underline{\mathbf{M}} = \overline{\rho} \frac{\partial \overline{\Phi}}{\partial \underline{\mathbf{K}}} = \overline{\rho} \frac{\partial \overline{\Phi}}{\partial \underline{\mathbf{K}}_{\mathrm{el}}}, \tag{46}$$

With (44) and (45), the macroscopic dissipation defined in (17) becomes

$$\overline{\rho D} = \underset{\sim}{\mathbf{\Sigma}} : \underset{\sim}{\mathbf{D}}_{\mathrm{pl}} + s \dot{\chi}_{\mathrm{pl}} + \underline{\mathbf{M}} \cdot \dot{\underline{\mathbf{K}}}_{\mathrm{pl}} \tag{47}$$

As in the original work of Gurson [14, 15], the potential $\overline{\Phi}(\underset{\sim}{\mathbf{E}}_{\mathrm{el}}, \chi_{\mathrm{el}}, \underline{\mathbf{K}}_{\mathrm{el}})$ is determined from a purely linear-elastic analysis wheres the evolution equations for the plastic behavior, i. e. yield condition and the associated flow rule, are derived from a limit load analysis for ideal rigid-plastic material.

3.2. Limit load analysis for rigid ideal-plastic material

For an ideal rigid-plastic material the microscopic specific dissipation is $\rho D = \underset{\sim}{\sigma} : \underset{\sim}{\mathbf{d}} =: \pi$. Thus, according to the definition (17) of the macroscopic dissipation as average of its microscopic counterpart, a limit-load analysis yields

$$\underset{\sim}{\mathbf{\Sigma}} : \underset{\sim}{\mathbf{D}} + s \dot{\chi} + \underline{\mathbf{M}} \cdot \dot{\underline{\mathbf{K}}} \leq \Pi \left(\underset{\sim}{\mathbf{D}}, \dot{\chi}, \dot{\underline{\mathbf{K}}} \right) := \inf \langle \pi \rangle_V \tag{48}$$

whereby the infinimum is taken over all kinematically admissible fields [1]. For a Mises material, the microscopic plastic dissipation is

$$\pi = \sigma_0 d_{\text{eq}} \qquad \text{with } d_{\text{eq}} = \sqrt{\frac{2}{3}\underset{\sim}{\mathbf{d}} : \underset{\sim}{\mathbf{d}}} \qquad \underset{\sim}{\mathbf{d}} = \left(\underline{\nabla}_{\underline{\mathbf{x}}}\underline{\mathbf{v}}\right)^{\text{S}} \tag{49}$$

Kinematically admissible are all incompressible fields

$$\underset{\sim}{\mathbf{d}} : \underset{\sim}{\mathbf{I}} = \underline{\nabla}_{\underline{\mathbf{x}}} \cdot \underline{\mathbf{v}} = 0 \tag{50}$$

which fulfill the kinematic micro-macro relations (20), (25) and (26) for prescribed values of the macroscopic deformation rates $\underset{\sim}{\mathbf{D}}$, $\dot{\chi}$ and $\dot{\underline{\mathbf{K}}}$. A subclass of this definition would incorporate only those fields which are additionally compatible with the kinematic boundary condition (32).

The yield surface is given in parametric form as

$$\underset{\sim}{\mathbf{\Sigma}} = \frac{\partial \Pi}{\partial \underset{\sim}{\mathbf{D}}}, \qquad s = \frac{\partial \Pi}{\partial \dot{\chi}}, \qquad \underline{\mathbf{M}} = \frac{\partial \Pi}{\partial \dot{\underline{\mathbf{K}}}}. \tag{51}$$

A common result (see e. g. [1]) for this type of models is that the yield surface $\Phi(\underset{\sim}{\mathbf{\Sigma}}, s, \underline{\mathbf{M}}) = 0$ is convex and the direction of plastic flow

$$\underset{\sim}{\mathbf{D}} = \lambda \frac{\partial \Phi}{\partial \underset{\sim}{\mathbf{\Sigma}}}, \qquad \dot{\chi} = \lambda \frac{\partial \Phi}{\partial s}, \qquad \dot{\underline{\mathbf{K}}} = \lambda \frac{\partial \Phi}{\partial \underline{\mathbf{M}}} \tag{52}$$

is orthogonal to it, whereby λ is the plastic multiplier.

3.3. Trial fields

With symmetric tensor $\underset{\sim}{\mathbf{D}}$, vector $\dot{\underline{\mathbf{K}}}$ and scalar $\dot{\chi}$, we have ten independent kinematic components which would require at least ten incompressible trial fields to cover them independently, i. e. at least four more than in Gurson's classical model. For the hollow sphere under consideration (Figure 1), the kinematic micro-macro relations for micro and macro dilatation, $\dot{\chi}$ and $\underset{\sim}{\mathbf{D}} : \underset{\sim}{\mathbf{I}}$, respectively, exhibit a spherical symmetry which is why this symmetry applies also to the respective trial fields. However, there is only a single incompressible field with spherical symmetry, namely that of Rice and Tracey [27] which is already among Gurson's classical trial fields. Thus, for an incompressible matrix there will be a kinematic constraint between the plastic parts of $\dot{\chi}$ and $\underset{\sim}{\mathbf{D}} : \underset{\sim}{\mathbf{I}}$. I. e., in addition to Gurson's trial velocity field, we need only an additional term $\underline{\mathbf{v}}_K(\underline{\xi})$ to account for the gradient $\dot{\underline{\mathbf{K}}}$ of the microdilatation:

$$\underline{\mathbf{v}}(\underline{\xi}) = A \frac{R^3}{r^3} \underline{\xi} + \underset{\sim}{\beta} \cdot \underline{\xi} + \underline{\mathbf{v}}_K(\underline{\xi}) \tag{53}$$

The incompressible matrix (50) requires $\underset{\sim}{\beta} : \underset{\sim}{\mathbf{I}} = 0$ for the field to be kinematically admissible. Due to the point symmetry/antisymmetry of the respective operators, the parameters A and $\underset{\sim}{\beta}$ can be determined independently of a specific choice of $\underline{\mathbf{v}}_K(\underline{\xi})$ if $\underline{\mathbf{v}}_K(-\underline{\xi}) = \underline{\mathbf{v}}_K(\underline{\xi})$. In particular, inserting (53) into the kinematic relations (20) and (41) yields

$$\dot{\chi}\underset{\sim}{\mathbf{D}} = \underset{\sim}{\beta} + A\underset{\sim}{\mathbf{I}} \tag{54}$$

As in the classical Gurson model, the coefficients can thus be linked to the deviatoric $\underset{\sim}{\beta} = \underset{\sim}{\mathbf{D}}^{\text{d}}$ and dilatational part $A = 1/3\underset{\sim}{\mathbf{D}} : \underset{\sim}{\mathbf{I}}$ of the macroscopic rate of deformation $\underset{\sim}{\mathbf{D}}$. Furthermore, (54) yields the kinematic constraint

$$\dot{\chi} = \frac{5}{2} \frac{1 - f^{2/3}}{1 - f^{5/3}} D_{\text{v}} \tag{55}$$

between the rates of microdilatation and macrodilatation, $\dot{\chi}$ and $D_{\mathrm{v}} = \underset{\sim}{\mathbf{D}} : \underset{\sim}{\mathbf{I}}$, respectively. The test field $\underline{\mathbf{v}}_K(\underline{\xi})$ of the gradient $\dot{\underline{\mathbf{K}}}$ of microdilatation needs to be linear and axially symmetric with respect to the vector $\dot{\underline{\mathbf{K}}}$ and incompressible. Thus, the approach of Gologanu et al. [12] is adopted and $\underline{\mathbf{v}}_K(\underline{\xi})$ is derived in terms of a Helmholtz decomposition. The condition of incompressibility (50) requires that $\underline{\mathbf{v}}_K(\underline{\xi})$ derives from a vector potential $\underline{\mathbf{\Psi}}(\underline{\xi})$:

$$\underline{\mathbf{v}}_K(\underline{\xi}) = \nabla \times \underline{\mathbf{\Psi}}(\underline{\xi})\,. \tag{56}$$

The axial symmetry with respect to $\dot{\underline{\mathbf{K}}}$ is ensured by choosing

$$\underline{\mathbf{\Psi}}(\underline{\xi}) = \dot{\underline{\mathbf{K}}} \times \underline{\xi}\, g_K(r) \tag{57}$$

According to (56), this corresponds to a velocity field

$$\underline{\mathbf{v}}_K(\underline{\xi}) = (2g_K + r g_K')\,\dot{\underline{\mathbf{K}}} - \frac{g_K'}{r}\underline{\xi}\,\underline{\xi}\cdot\dot{\underline{\mathbf{K}}}\,. \tag{58}$$

Obviously, a constant value of the yet undetermined function $g_K(r)$ corresponds to a pure rigid body translation in direction of $\dot{\underline{\mathbf{K}}}$. The macroscopic velocity (37) associated with the field (58) amounts to

$$\underline{\mathbf{V}}(\underline{\mathbf{X}}) = \frac{2}{1-f}\dot{\underline{\mathbf{K}}}\left[g_K(R) - f g_K(R_{\mathrm{void}})\right]\,. \tag{59}$$

Inserting the field (58) into to the kinematic micro-macro relation (26) leads to[3]

$$\dot{\underline{\mathbf{K}}} = -\frac{3}{2R^2}\dot{\underline{\mathbf{K}}}\left[R g_K'(R) + \frac{2f}{1-f}\left[g_K(R) - g_K(R_{\mathrm{void}})\right]\right] \tag{60}$$

Thus, it is required that the square bracket in (60) equals $-2/3R^2$.

The macroscopic plastic dissipation (48) is bounded from above as in most Gurson-type models by

$$\Pi = \sigma_0 \frac{3}{R^3} \int\limits_{R_{\mathrm{void}}}^{R} r^2 \sqrt{\frac{2}{3}\left\langle \underset{\sim}{\mathbf{d}} : \underset{\sim}{\mathbf{d}} \right\rangle_{S(r)}}\mathrm{d}r\,. \tag{61}$$

For the velocity field (58), this upper bound value becomes

$$\Pi = \sigma_0 \frac{3}{R^3} \int\limits_{R_{\mathrm{void}}}^{R} r^2 \sqrt{\left(4A^2\frac{R^6}{r^6} + \frac{2}{3}\underset{\sim}{\beta} : \underset{\sim}{\beta} + \frac{2}{9}\dot{\underline{\mathbf{K}}}\cdot\dot{\underline{\mathbf{K}}}\left[10(g_K')^2 + (r g_K'')^2 + 4 r g_K' g_K''\right]\right)}\mathrm{d}r\,. \tag{62}$$

The first derivative $g_K'(r)$ dominates the term with the gradient $\dot{\underline{\mathbf{K}}}$ of microdilatation until the void volume fraction is not too small. Consequently, a linear ansatz is chosen for $g_K(r)$. Thus, (60) leads to

$$g_K(r) = \frac{2}{3}R^2\frac{1-f^{5/3}}{1-f} - \frac{2}{3}R\frac{1-f}{1+f-2f^{4/3}}\,r \tag{63}$$

whereby the offset value was chosen arbitrarily such that the macroscopic velocity $\underline{\mathbf{V}}$ according to (59) vanishes. The trial field $\underline{\mathbf{v}}_K(\underline{\xi})$ with linear ansatz (63) is visualized in Figure 2. The linear ansatz (63) has the advantage that the contribution of the $\dot{\underline{\mathbf{K}}}$ term to the radicand in (62) is a constant so that the

[3] As in [23] solely requirement (26) is imposed and not the kinematic boundary conditions (32). The latter would imply the additional requirement $g_K'(R) = -R/3$.

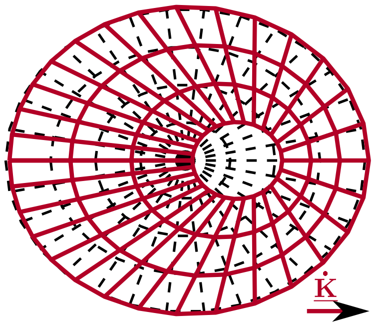

Figure 2: Trial field $\underline{\mathbf{v}}_K(\underline{\xi})$ (vector $\underline{\mathbf{K}}$ in horizontal direction)

integral in (62) can be solved exactly preserving the rigorous upper-bound character of the solution. The integral yields

$$\Pi(\alpha, B_{\mathrm{eq}}) = \alpha\sigma_0 B_{\mathrm{eq}} \int\limits_{\alpha}^{\alpha/f} \frac{\sqrt{1+w^2}}{w^2}\mathrm{d}w \qquad = \alpha\sigma_0 B_{\mathrm{eq}} \left[\operatorname{arcsinh}(w) - \frac{\sqrt{1+w^2}}{w} \right]_{w=\alpha}^{\alpha/f} \tag{64}$$

whereby the abbreviations

$$w = \alpha\,(R/r)^3 \quad \text{with} \quad \alpha = 2A/B_{\mathrm{eq}} \tag{65}$$

$$B_{\mathrm{eq}}^2 = \frac{2}{3}\underset{\sim}{\mathbf{D}}^{\mathrm{d}} : \underset{\sim}{\mathbf{D}}^{\mathrm{d}} + \frac{R^2}{q_M}\dot{\underline{\mathbf{K}}} \cdot \dot{\underline{\mathbf{K}}} \quad \text{with} \quad q_M = \frac{81}{80}\left(\frac{1+f-2f^{4/3}}{1-f}\right)^2 \tag{66}$$

were introduced.

3.4. Yield function

For obtaining the yield locus, the macroscopic plastic dissipation Π in (51) needs to be amended by the kinematic constraint (55) which is enforced by a Lagrange multiplier λ_{v}:

$$\widetilde{\Pi} = \Pi + \lambda_{\mathrm{v}} \left[\dot{\chi} - \frac{5}{2}\frac{1-f^{2/3}}{1-f^{5/3}} D_{\mathrm{v}} \right] \tag{67}$$

The parametric form of the macroscopic yield surface is obtained according to (51) from $\widetilde{\Pi}$. Firstly, inserting (67) to the corresponding relation for the microdilatation

$$s = \frac{\partial \widetilde{\Pi}}{\partial \dot{\chi}} = \lambda_{\mathrm{v}} \tag{68}$$

shows that the Lagrange multiplier corresponds to the microdilatational stress difference. With this finding, the remaining relations from (51) read

$$\underset{\sim}{\boldsymbol{\Sigma}} = \frac{\partial \widetilde{\Pi}}{\partial \underset{\sim}{\mathbf{D}}} = \underbrace{\left(\frac{\partial \Pi}{\partial B_{\mathrm{eq}}} - \frac{\alpha}{B_{\mathrm{eq}}}\frac{\partial \Pi}{\partial \alpha} \right)}_{=:Q} \frac{\frac{2}{3}\underset{\sim}{\mathbf{D}}^{\mathrm{d}}}{B_{\mathrm{eq}}} + \underbrace{\frac{2}{3}\frac{1}{B_{\mathrm{eq}}}\frac{\partial \Pi}{\partial \alpha}}_{=:P} \underset{\sim}{\mathbf{I}} - s\,\frac{5}{2}\frac{1-f^{2/3}}{1-f^{5/3}}\underset{\sim}{\mathbf{I}}, \tag{69}$$

$$\underline{\mathbf{M}} = \frac{\partial \widetilde{\Pi}}{\partial \dot{\underline{\mathbf{K}}}} = \left(\frac{\partial \Pi}{\partial B_{\mathrm{eq}}} + \frac{\partial \Pi}{\partial \alpha}\frac{\partial \alpha}{\partial B_{\mathrm{eq}}} \right) \frac{\partial B_{\mathrm{eq}}}{\partial \dot{\underline{\mathbf{K}}}} = Q\frac{R^2}{q_M}\frac{\dot{\underline{\mathbf{K}}}}{B_{\mathrm{eq}}}\,. \tag{70}$$

In order to get an implicit expression, the quantities Q and P (which correspond to Mises stress and hydrostatic stress in Gurson's original model, respectively) need to be expressed in terms of the stresses $\underset{\sim}{\mathbf{\Sigma}}$, s and $\underline{\mathbf{M}}$. For the hydrostatic part of (69) this is

$$P = \frac{1}{3}\underset{\sim}{\mathbf{\Sigma}} : \underset{\sim}{\mathbf{I}} + \frac{5}{2}\frac{1 - f^{2/3}}{1 - f^{5/3}} s \tag{71}$$

whereas a close look on the deviatoric part of (69) and (70) in the light of (66) shows that

$$Q^2 = \frac{3}{2}\underset{\sim}{\mathbf{\Sigma}}^{\mathrm{d}} : \underset{\sim}{\mathbf{\Sigma}}^{\mathrm{d}} + \frac{q_M}{R^2}\underline{\mathbf{M}} \cdot \underline{\mathbf{M}} \,. \tag{72}$$

The parameters α and B_{eq} of the implicit description $Q(\alpha, B_{\mathrm{eq}})$ and $P(\alpha, B_{\mathrm{eq}})$ can now be eliminated as in Gurson's original model. Finally, the yield function becomes

$$\Phi = \frac{Q^2}{\sigma_0^2} + 2f\cosh\left(\frac{3}{2}\frac{P}{\sigma_0}\right) - (1 + f^2) \tag{73}$$

It can easily verified that an associated flow rule (52) and Φ with P in form of (71) satisfy the kinematic constraint (55).

3.5. Elastic behavior

For obtaining the macroscopic elastic properties of the microdilatational contiuum, the boundary value problem outlined in sections 2.4 and 2.5, respectively, has to be solved for elastic material behavior of the matrix material. In particular, isotropic linear elastic behavior $\underset{\sim}{\sigma} = 2\mu^{(\mathrm{m})}\underset{\sim}{\varepsilon} + \lambda^{(\mathrm{m})}\underset{\sim}{\mathbf{I}}\,\underset{\sim}{\varepsilon} : \underset{\sim}{\mathbf{I}}$ of the matrix material is considered corresponding to a specific mechanical intrinsic energy $\rho\Phi = \mu^{(\mathrm{m})}\underset{\sim}{\varepsilon} : \underset{\sim}{\varepsilon} + 1/2\lambda^{(\mathrm{m})}(\underset{\sim}{\varepsilon} : \underset{\sim}{\mathbf{I}})^2$. Together with the isotropy of the spherical ΔV, the mechanical part of the macroscopic intrinsic energy (45) thus decomposes for symmetry reasons as

$$\overline{\rho}\overline{\Phi} = \mu^{(\mathrm{eff})}\underset{\sim}{\mathbf{E}}^{\mathrm{d}}_{\mathrm{el}} : \underset{\sim}{\mathbf{E}}^{\mathrm{d}}_{\mathrm{el}} + \frac{1}{2}K^{(\mathrm{eff})}_{\varepsilon}\left(\underset{\sim}{\mathbf{E}}_{\mathrm{el}} : \underset{\sim}{\mathbf{I}}\right)^2 + \frac{1}{2}K^{(\mathrm{eff})}_{\chi}\chi^2_{\mathrm{el}} + K^{(\mathrm{eff})}_{\varepsilon\chi}\underset{\sim}{\mathbf{E}}_{\mathrm{el}} : \underset{\sim}{\mathbf{I}}\,\chi_{\mathrm{el}} + \frac{1}{2}\gamma^{(\mathrm{eff})}\underline{\mathbf{K}}_{\mathrm{el}} \cdot \underline{\mathbf{K}}_{\mathrm{el}} \,. \tag{74}$$

According to (46), the state law for the stress measures becomes

$$\begin{aligned}
\underset{\sim}{\mathbf{\Sigma}} &= \overline{\rho}\frac{\partial\overline{\Phi}}{\partial\underset{\sim}{\mathbf{E}}_{\mathrm{el}}} = 2\mu^{(\mathrm{eff})}\underset{\sim}{\mathbf{E}}^{\mathrm{d}}_{\mathrm{el}} + \left(K^{(\mathrm{eff})}_{\varepsilon}\underset{\sim}{\mathbf{E}}_{\mathrm{el}} : \underset{\sim}{\mathbf{I}} + K^{(\mathrm{eff})}_{\varepsilon\chi}\chi_{\mathrm{el}}\right)\underset{\sim}{\mathbf{I}}, \\
s &= \overline{\rho}\frac{\partial\overline{\Phi}}{\partial\chi_{\mathrm{el}}} = K^{(\mathrm{eff})}_{\chi}\chi_{\mathrm{el}} + K^{(\mathrm{eff})}_{\varepsilon\chi}\underset{\sim}{\mathbf{E}}_{\mathrm{el}} : \underset{\sim}{\mathbf{I}}, \\
\underline{\mathbf{M}} &= \overline{\rho}\frac{\partial\overline{\Phi}}{\partial\underline{\mathbf{K}}_{\mathrm{el}}} = \gamma^{(\mathrm{eff})}\underline{\mathbf{K}}_{\mathrm{el}},
\end{aligned} \tag{75}$$

The macroscopic shear modulus $\mu^{(\mathrm{eff})}$ can be determined by classical methods whose results can be found in textbooks. The three constants $K^{(\mathrm{eff})}_{\varepsilon}$, $K^{(\mathrm{eff})}_{\chi}$ and $K^{(\mathrm{eff})}_{\varepsilon\chi}$ can be determined exactly from Navier's solution of a hollow sphere as shown in detail in appendix A.1. Note that $K^{(\mathrm{eff})}_{\varepsilon}$ is *not* the macroscopic bulk modulus. Rather, for a macroscopically uniform deformation, the higher order balance of momentum (13) requires (in absence of volume loads and inertia) that $s = 0$. Thus, $(75)_2$ gives a relation between (the elastic parts of) micro and macrodilatation. Solving for the microdilatation χ_{el} and inserting this value to $(75)_1$ shows that the macroscopic bulk modulus is $K^{(\mathrm{eff})} = K^{(\mathrm{eff})}_{\varepsilon} - (K^{(\mathrm{eff})}_{\varepsilon\chi})^2/K^{(\mathrm{eff})}_{\chi}$.

For determining the coefficient $\gamma^{(\mathrm{eff})}$ of the gradient term, an axisymmetric linear boundary value problem has to be solved. Here, for simplicity an approximate solution is constructed by the Rayleigh–Ritz method. Suitable trial fields could be the incompressible ansatz (58) with (63) from the limit load analysis or to extend the quadratic field $\underline{\mathbf{u}} = 1/3\underset{\sim}{\xi}\underline{\mathbf{K}} \cdot \underset{\sim}{\xi}$ from the essential BC (43) to the complete domain

$\underline{\mathbf{x}} \in \Delta V$ as in [17]. It turns out that for an elastically compressible matrix, the latter leads to a lower elastic energy, i. e. to a better result, and the elastic gradient coefficient can be estimated as

$$\gamma^{(\mathrm{eff})} = 2\left[7\mu^{(\mathrm{m})} + 8\lambda^{(\mathrm{m})}\right]\frac{1-f^{5/3}}{45}R^2\,. \tag{76}$$

4. Heuristic extensions

In a strict sense, Gurson's yield function applies to rigid ideal-plastic material only. It is thus of little practical use until several heuristic extensions are introduced. Of course, this is the case for its microdilatational extension as well which is why several established extensions shall be discussed and adapted to the present microdilatational model. Most significant are presumably the extensions to elastic-plastic behavior, to work-hardening and to the evolution of the void volume fraction f, which were proposed by Gurson [14] himself. Isotropic hardening is incorporated by replacing the matrix yield stress σ_0 in yield function (73) by some effective value $\bar{\sigma} = \bar{\sigma}(\varepsilon_{\mathrm{eq}})$ which is postulated to be a function of the equivalent accumulated plastic strain $\varepsilon_{\mathrm{eq}}$. The evolution of $\varepsilon_{\mathrm{eq}}$ is driven by the macroscopic plastic dissipation. For the microdilatational model (47) changedwith flow rule (52) and a yield function Φ in the form of (73), the evolution equation becomes

$$\dot{\varepsilon}_{\mathrm{eq}} = \frac{1}{(1-f)\bar{\sigma}}\left(\underset{\sim}{\mathbf{\Sigma}} : \underset{\sim}{\mathbf{D}}_{\mathrm{pl}} + s\dot{\chi}_{\mathrm{pl}} + \underline{\mathbf{M}}\cdot\underline{\dot{\mathbf{K}}}_{\mathrm{pl}}\right) = \lambda\frac{\frac{\partial\Phi}{\partial Q}Q + \frac{\partial\Phi}{\partial P}P}{(1-f)\bar{\sigma}}\,. \tag{77}$$

The evolution equation of f

$$\dot{f} = (1-f)D_{\mathrm{v}} + \dot{f}_{\mathrm{N}} \tag{78}$$

can be adapted one-by-one from Gurson. The growth term $\dot{f}_{\mathrm{G}} = (1-f)D_{\mathrm{v}}$ was derived from the condition of plastic incompressibility of the matrix. Note that the rate of microdilatation $\dot{\chi}_{\mathrm{pl}}$ is linked to the macroscopic plastic dilatation D_{v} by the kinematic constraint (55), which could be inserted equivalently to (78). The incompressibility of the matrix implies also the evolution equation

$$\dot{R} = \frac{R}{3}\underset{\sim}{\mathbf{D}}_{\mathrm{pl}} : \underset{\sim}{\mathbf{I}} \tag{79}$$

of the intrinsic length R which is to be interpreted as mean half-distance of voids.

Without any problem, the models of continuous strain-controlled void nucleation by Chu and Needleman [5] or by Zhang [30] can be used for $\dot{f}_{\mathrm{N}}$. In this case the intrinsic length R is to be interpreted as the mean of the half distance of potential nuclei. The adaption of stress-controlled nucleation would require to specify the roles of the additional stress measures s and $\underline{\mathbf{M}}$ on this process, in the simplest case they are neglected.

the

Although the derivation of the yield function (73) ensures that it is a rigorous bound for rigid ideal-plastic matrix material, for practical applications it is more relevant to improve the predictive quality of the model for elastic-plastic material with hardening. For this purpose, Tvergaard [28] introduced the parameters q_1 and q_2 and replaced in the Gurson yield function f by $q_1 f$ and P by $q_2 P$, respectively. Extensive parameter studies with cell models were performed in literature, see e. g. [9]. Although such cell models did not incorporate the non-classical macroscopic deformation measures of the present theory, the classical theory and thus the performed cell model simulations are a special case of the microdilatational framework and should therefore be captured adequately as well. For this reason it seems reasonable to introduce q_1 and q_2 and their particular values also in the microdilatational yield function (73). In this context, it suggests itself to calibrate the coefficient q_M of the hyperstress term to respective cell model simulations with non-vanishing gradient $\underline{\mathbf{K}}$ of microdilatation. Gologanu et al. [12] performed cell model simulations for their extension of Gurson's model to the strain gradient theory. Although the macroscopic framework of their theory exhibits some differences to the present one, the quadratic term of the kinematic boundary conditions which they applied at the microscale for the dilatational part is identical to the corresponding term in (43) of the present contribution, up to a factor of 1/3. Thus, the results of the cell model computations by Gologanu et al. [12] can be used directly for calibrating q_M. In particular, a comparison of the respective generalized Hill-Mandel lemmas in context of the mentioned quadratic part of the microscopic boundary condition shows that the calibration parameter Δ_{CC} of [12], which was identified as $1.58 \lesssim \Delta_{CC} \lesssim 1.71$ for small porosities $f \leq 0.01$, can directly related to the present model as $q_M = 9/\Delta_{CC}$. It shall not be concealed, that the difference between these calibrated values and the q_M of the present limit load analysis is significant indicating that the trial field (63), which was chosen for convenience to be able to solve the integral in (62) in closed form, may be improved.

The last class of heuristic extensions addresses the modeling of void coalescence. The most prominent representative thereof is surely the model of Tvergaard and Needleman [29] wherein the void volume fraction f in the yield function is replaced by f^*. The effective void volume fraction f^* coincides with the actual one f until f reaches f_c and coalescence is assumed to initiate. In the coalescence stage, f^* increases faster then f does according to (78). The Tvergaard-Needleman coalescence model can be adapted to the present extension of Gurson's model since it ensures that the macroscopic softening is driven only by dilatational deformations which are regularized by the microdilatational theory[4]. Recently, coalescence models of Thomason-type attracted research activities (for a recent review the reader is referred to Benzerga et al. [2]). If they are implemented as a second yield condition they are not suitable for the present microdilatational framework since softening can then be driven also by deviatoric deformations. For the same reason the shear modification of Nahshon and Hutchinson [24] is inadequate. However, well-suited for the microdilatational model is the approach of Zhang [30] to implement the approach of Tvergaard and Needleman [29] with f_c determined from Thomason's criterion (or one of its recent enhancements) in dependence of the current stress state.

5. Summary, conclusions and outlook

In the present contribution, Gurson's model of ductile material degradation is extended towards the theory of microdilatational media. For this purpose, the theory of micromorphic homogenization for compact media [16] is confined to the special case of microdilatational continua and extended towards porous media. As in Gurson's original work, the yield function is obtained from a limit load analysis for ideal rigid-plastic matrix material of Mises type. In order to identify the contribution of the hyperstresses to the yield function, additional trial fields from the family of Gologanu et al. [12] are adapted. Consequently, the hyperstresses enter the resulting yield function as in [12] together with an intrinsic length. Compared to the strain-gradient theory of [12], the so-called difference stress enters additionally the yield function in the present microdilatational model. As usual the model is extended towards elastic-plastic behavior by postulating an additive split of all deformation measures into elastic and plastic parts. The elastic moduli of the non-classical terms are determined in closed form by homogenization as well. It turned out that the microscopic plastic incompressibility of the matrix material implies a constraint between the plastic parts of microdilatation and macroscopic dilatation whereas the elastic parts of both quantities differ in general. That is why the model falls into the class of unconstrained micromorphic continua which are well-suited for an implementation into standard finite element codes. Several established heuristic extensions of Gurson's model, in particular regarding hardening and void coalescence are discussed and adapted to the microdilatational model.

Future finite element implementations and corresponding simulations have to show whether the developed model can combine computational efficiency with predictive capabilities of the model of Gologanu et al. [12] as envisaged. Definitively, the developed model will be adequate only in situations when

[4]Strictly speaking, the nucleation term in (78) may violate this condition. However, this is of no practical relevance if the nucleation parameters are chosen such that the nucleation occurs mainly before reaching f_c.

softening is driven by void growth and the associated dilatation, i. e. for medium to high levels of stress triaxiality (a restriction which applies to Gurson's model as well). Under low levels of stress triaxiality, the change of void shape becomes relevant. A challenging future task will be to develop a fully micromorphic model which incorporates void shape effects.

A. Appendix

A.1. Elastic solution for hollow sphere

For isotropic linear elastic behavior and spherical-symmetrical loading, the Lamé equation [see e. g. 20] to (38) for the hollow sphere (Figure 1) becomes (with geometric moment from (40))

$$\left(\frac{1}{r^2}(r^2 u)'\right)' = -\frac{5}{(1-f^{5/3})R^2}\,\frac{s}{2\mu^{(\mathrm{m})}+\lambda^{(\mathrm{m})}}\,r \tag{80}$$

with displacements $\underline{\mathbf{u}} = u(r)\underline{\mathbf{b}}_r$. Integrating this ODE yields

$$u(r) = -\frac{1}{2}\,\frac{1}{1-f^{5/3}}\,\frac{s}{2\mu^{(\mathrm{m})}+\lambda^{(\mathrm{m})}}\,\frac{r^3}{R^2} + c_1 r + c_2\frac{R^3}{r^2} \tag{81}$$

with two constants of integration c_1 and c_2 (containing, by the way, the Rice and Tracey field as in (53)). The corresponding radial stresses are

$$\sigma_{rr} = -\frac{1}{2}\,\frac{1}{1-f^{5/3}}\,\frac{6\mu^{(\mathrm{m})}+5\lambda^{(\mathrm{m})}}{2\mu^{(\mathrm{m})}+\lambda^{(\mathrm{m})}}\,\frac{r^2}{R^2}s + \left(2\mu^{(\mathrm{m})}+3\lambda^{(\mathrm{m})}\right)c_1 - 4\mu^{(\mathrm{m})}c_2\frac{R^3}{r^3} \tag{82}$$

For the hollow sphere under spherical-symmetrical loading, the kinematic and kinetic micro-macro relations (33), (41) and (11), respectively, become

$$E_\mathrm{v} := \underset{\sim}{\mathbf{E}} : \underset{\sim}{\mathbf{I}} = \frac{3}{R}u(R), \qquad \chi = \frac{15}{R^5}\,\frac{1}{1-f^{5/3}}\int\limits_{R_\mathrm{void}}^{R} r^3 u(r)\mathrm{d}r, \qquad \Sigma_\mathrm{h} := \frac{1}{3}\underset{\sim}{\mathbf{\Sigma}} : \underset{\sim}{\mathbf{I}} = \sigma_{rr}(r=R) \tag{83}$$

For the ODE (80) it makes no difference whether $(83)_1$ or $(83)_3$ is applied as kinematic or static boundary condition (32) or (31), respectively. For simplicity, the constants of integration c_1 and c_2 are determined firstly by $(83)_3$ together with the natural boundary condition $\sigma_{rr}(r = R_\mathrm{void}) = 0$ at the void surface. With these values, the kinematic relations $(83)_1$ or $(83)_2$ become

$$E_\mathrm{v} = \underbrace{\frac{1}{K}\,\frac{1}{1-f}\left[1+\frac{f}{2}\,\frac{1+\nu}{1-2\nu}\right]}_{=:\kappa_1}\Sigma_\mathrm{h} + \underbrace{\frac{1}{K}\,\frac{1}{1-f}\left[1+\frac{f}{2}\,\frac{1+\nu}{1-2\nu}\,\frac{5}{2}\,\frac{1-f^{2/3}}{1-f^{5/3}}\right]}_{=:\kappa_{21}} s \tag{84}$$

$$\begin{aligned}\chi &= \underbrace{\frac{1}{K}\,\frac{1}{1-f}\left[1+\frac{f}{2}\,\frac{1+\nu}{1-2\nu}\,\frac{5}{2}\,\frac{1-f^{2/3}}{1-f^{5/3}}\right]}_{=:\kappa_{12}}\Sigma_\mathrm{h} \\ &\quad + \underbrace{\frac{1}{2K}\,\frac{1}{1-f}\,\frac{3-\nu}{1-\nu}\left[1+\frac{f}{2}\,\frac{1+\nu}{1-2\nu}\left(\frac{1-f^{2/3}}{1-f^{5/3}}\right)^2 - \frac{1+\nu}{3-\nu}\,\frac{5}{7}\,\frac{1-f^{7/3}}{1-f^{5/3}}\,\frac{1-f}{1-f^{5/3}}\right]}_{=:\kappa_2} s \\ &= \underbrace{\frac{1}{K}\,\frac{1}{1-f}\left[1+\frac{f}{2}\,\frac{1+\nu}{1-2\nu}\,\frac{5}{2}\,\frac{1-f^{2/3}}{1-f^{5/3}}\right]}_{=:\kappa_{12}}\Sigma_\mathrm{h} + \underbrace{\frac{1}{K}\,\frac{1}{1-f}\,\frac{2}{7}\,\frac{4-3\nu}{1-\nu}\left[1+f\frac{25}{16}\,\frac{5-3\nu}{4-3\nu}\,\frac{1+\nu}{1-2\nu}\,\frac{\left(1-f^{2/3}\right)^2}{\left(1-f^{5/3}\right)^2}\right]}_{=:\kappa_2} s\end{aligned} \tag{85}$$

wherein $K = 2\mu^{(\mathrm{m})}/3 + \lambda^{(\mathrm{m})}$ is the bulk modulus of the matrix. As necessary for the existence of a thermodynamic potential, the crossed coefficients are equal, $\kappa_{21} = \kappa_{12}$, due to the consistent kinetic and kinematic micro-macro relations. Inverting (84)–(85) for Σ_h and s and comparing with $(75)_1$ and $(75)_2$ shows that the macroscopic elastic stiffness coefficients are

$$K_\varepsilon^{(\mathrm{eff})} = \frac{\kappa_2}{\kappa_2\kappa_1 - \kappa_{12}^2}, \qquad K_\chi^{(\mathrm{eff})} = \frac{\kappa_1}{\kappa_2\kappa_1 - \kappa_{12}^2}, \qquad K_{\varepsilon\chi}^{(\mathrm{eff})} = -\frac{\kappa_{12}}{\kappa_2\kappa_1 - \kappa_{12}^2} \tag{86}$$

and that the macroscopic bulk modulus according to the discussion in section 3.5 is $K^{(\mathrm{eff})} = K_\varepsilon^{(\mathrm{eff})} - (K_{\varepsilon\chi}^{(\mathrm{eff})})^2/K_\chi^{(\mathrm{eff})} = 1/\kappa_1$, corresponding just to (84) reduced to the classical case $s = 0$. For vanishing porosity $f = 0$, the coefficients in (86) become $K_\chi^{(\mathrm{eff})} = -K_{\varepsilon\chi}^{(\mathrm{eff})} = 7(1-\nu)/(1+\nu)K$ and $K_\varepsilon^{(\mathrm{eff})} = K + K_\chi^{(\mathrm{eff})}$ and the effective bulk modulus becomes identical to the matrix value $K^{(\mathrm{eff})} = K$.

References

[1] Benzerga, A. A., Leblond, J.-B., 2010. Ductile fracture by void growth to coalescence. Adv. Appl. Mech. 44, 169–305.

[2] Benzerga, A. A., Leblond, J.-B., Needleman, A., Tvergaard, V., 2016. Ductile failure modeling. Int. J. Fracture. 201, 29–80.

[3] Bergheau, J.-M., Leblond, J.-B., Perrin, G., 2014. A new numerical implementation of a second-gradient model for plastic porous solids, with an application to the simulation of ductile rupture tests. Comput. Method. Appl. M. 268, 105–125.

[4] Besson, J., 2010. Continuum models of ductile fracture: A review. Int. J. Damage. Mech. 19 (1), 3–52.

[5] Chu, C. C., Needleman, A., 1980. Void nucleation effects in biaxially stretched sheets. J. Eng. Mater-T. Asme. 102 (3), 249–256.

[6] Enakoutsa, K., Leblond, J.-B., 2009. Numerical implementation and assessment of the GLPD micromorphic model of ductile rupture. Eur. J. Mech. A-Solid. 28 (3), 445–460.

[7] Eringen, A. C., 1968. Mechanics of micromorphic continua. In: Mechanics of Generalized Continua: Proceedings of the IUTAM-Symposium on The Generalized Cosserat Continuum and the Continuum Theory of Dislocations with Applications, Freudenstadt and Stuttgart (Germany) 1967. Springer, Berlin, Heidelberg, pp. 18–35.

[8] Eringen, A. C., Suhubi, E. S., 1964. Nonlinear theory of simple micro-elastic solids–i. Int. J. Eng. Sci. 2 (2), 189–203.

[9] Faleskog, J., Gao, X., Shih, C. F., 1998. Cell model for nonlinear fracture analysis – i. micromechanics calibration. Int. J. Fracture. 89 (4), 355–373.

[10] Forest, S., 2009. Micromorphic approach for gradient elasticity, viscoplasticity, and damage. J. Eng. Mech. 135 (3), 117–131.

[11] Forest, S., Sievert, R., 2006. Nonlinear microstrain theories. Int. J. Solids Struct. 43 (24), 7224–7245.

[12] Gologanu, M., Leblond, J. B., Perrin, G., Devaux, J., 1997. Recent extensions of Gurson's model for porous ductile metals – part II: A Gurson-like model including the effect of strong gradients of the macroscopic field. In: Suquet, P. (Ed.), Continuum micromechanics. No. 377 in CISM Courses And Lectures. Springer-Verlag, New York, pp. 97–130.

[13] Goodman, M. A., Cowin, S. C., 1972. A continuum theory for granular materials. Arch. Ration. Mech. An. 44 (4), 249–266.

[14] Gurson, A. L., 1975. Plastic flow and fracture behavior of ductile materials incorporating void nucleation, growth, and interaction. Phd thesis, Brown University.

[15] Gurson, A. L., 1977. Continuum theory of ductile rupture by void nucleation and growth: Part i – yield criteria and flow rules for porous ductile media. J. Eng. Mater-T. Asme. 99 (1), 2–15.

[16] Hütter, G., 2017. Homogenization of a Cauchy continuum towards a micromorphic continuum. J. Mech. Phys. Solids 99, 394–408.

[17] Hütter, G., Mühlich, U., Kuna, M., 2015. Micromorphic homogenization of a porous medium: elastic behavior and quasi-brittle damage. Contin. Mech. Therm. 27, 1059–1072.

[18] Jackiewicz, J., Kuna, M., 2003. Non-local regularization for FE simulation of damage in ductile materials. Comp. Mater. Sci. 28 (3–4), 684–695.

[19] Jänicke, R., Steeb, H., 2012. Minimal loading conditions for higher order numerical homogenisation schemes. Arch. Appl. Mech. 82 (8), 1075–1088.

[20] Kachanov, M., Shafiro, B., Tsukrov, I., 2003. Handbook of elasticity solutions. Kluwer Academic Publishers, Dordrecht / Boston / London.

[21] Leblond, J. B., Perrin, G., Devaux, J., 1994. Bifurcation effects in ductile metals with nonlocal damage. J. Appl. Mech. 61 (2), 236–242.

[22] Linse, T., Hütter, G., Kuna, M., 2012. Simulation of crack propagation using a gradient-enriched ductile damage model based on dilatational strain. Eng. Fract. Mech. 95, 13–28.

[23] Monchiet, V., Charkaluk, E., Kondo, D., 2011. A micromechanics-based modification of the Gurson criterion by using Eshelby-like velocity fields. Eur. J. Mech. A-Solid. 30 (6), 940–949.

[24] Nahshon, K., Hutchinson, J. W., 2008. Modification of the Gurson model for shear failure. Eur. J. Mech. A-Solid. 27 (1), 1–17.

[25] Needleman, A., Tvergaard, V., 1998. Dynamic crack growth in a nonlocal progressively cavitating solid. Eur. J. Mech. A-Solid. 17 (3), 421–438.

[26] Reusch, F., Svendsen, B., Klingbeil, D., 2003. Local and non-local Gurson-based ductile damage and failure modelling at large deformation. Eur. J. Mech. A-Solid. 22 (6), 779–792.

[27] Rice, J. R., Tracey, D. M., 1969. On the ductile enlargement of voids in triaxial stress fields. J. Mech. Phys. Solids 17 (3), 201–217.

[28] Tvergaard, V., 1981. Influence of voids on shear band instabilities under plane strain conditions. Int. J. Fracture. 17 (4), 389–407.

[29] Tvergaard, V., Needleman, A., 1984. Analysis of the cup-cone fracture in a round tensile bar. Acta. Metall. Mater. 32 (1), 157–169.

[30] Zhang, Z. L., 2001. A complete Gurson model. In: Aliabadi, M. H. (Ed.), Nonlinear Fracture & Damage Mechanics. WITpress, Southhampton, Boston, Ch. 8, pp. 223–248.